Journal of Sound and Vibration (2001) **242**(1), 125–150
doi:10.1006/jsvi.2000.3364, available online at http://www.idealibrary.com on IDEAL®

TWO GENERALIZED HIGHER ORDER THEORIES IN FREE VIBRATION STUDIES OF MULTILAYERED PLATES

A. MESSINA

Dipartimento di Ingegneria dell'Innovazione, Università di Lecce, Via Monteroni, 73100 *Lecce, Italy*.
E-mail: *arcangelo.messina@unile.it*

(*Received* 10 *April* 2000, *and in final form* 13 *September* 2000)

This paper presents an extension of two-dimensional models for the analysis of freely vibrating laminated plates. The extension concerns the enlargement of higher order theories, recently introduced by different authors in several forms, to encompass higher order terms over the cubic one usually taken into consideration. Higher order effects such as rotatory inertia and transverse shear stress are naturally included without any shear correction factors. Namely, two different models are introduced by expanding, on different functional bases, displacements (D2D) and transverse shear stresses in conjunction with displacements (M2D). The expansion is considered to be consistent with the traction-type boundary condition on the external surfaces of the plate. The governing equations and associated boundary conditions are consistently obtained by the classical Hamilton's variational principle and Reissner's mixed variational theorem. Both models are equivalent single layer type and, therefore, differ according to the layer-wise descriptions, preserve the independence of the number of unknown variables on the number of layers. However, this feature is presented together with intrinsic physical violations for both models. Model D2D violates the interlaminar stress continuity requirement and model M2D violates in a weaker from the same requirement (derivatives are not piecewise continuous), besides neglecting the transverse normal stress. The importance of completely fulfilling the mentioned continuity is then discussed once the relevant governing equations are tailored for the cylindrical bending condition. The effectiveness of the models is indicated by making numerical comparisons with the exact three-dimensional theory of the elasticity for several lamination schemes, angle/cross-ply lay-ups, and characteristic geometric ratios for low and higher frequencies.

1. INTRODUCTION

Laminated plates and shells are widely used in several engineering fields such as aircraft, automobiles, marine and submarine vehicles besides other industrial applications. Consequently, these applications have stimulated interest in introducing corresponding mathematical models to predict the dynamical behaviour of the physical models with sufficient accuracy. Moreover, composite laminated plates and shells have great importance in modeling many of the mechanical parts employed in several systems, particularly where optimized strength/weight ratios are required. As far as this work is concerned two analytical models are formulated in an attempt to generalize some documented and tested two-dimensional theories [1–11] where free vibration studies are involved. The attention given to this particular global response of structural elements is largely justified by the engineering applications involving these modal data [12, 13].

In the kind of generalization we are dealing with, normal effects (in terms of displacements and/or stresses) are neglected. In this respect, this work should be mainly

0022-460X/01/160125 + 26 $35.00/0

compared with recent studies [14–16], where this influence was not accounted for, and for which the effect of lamination schemes, boundary conditions, geometric characteristics, different materials on natural frequencies was investigated. In particular, recent references [14, 15] studied the influence of boundary conditions on modal parameters related to the free vibration of shells and plates. Besides the valuable numerical results presented in those works, some dynamical behaviours were not completely clarified and for this reason they were considered as an issue for further investigation. As far as the modelling is concerned in references [14, 15], particular emphasis was given to a parabolic shear deformable shell theory [17, 18] accounting for the continuity of interlaminar stresses. The natural frequencies coming from this theory (PAR_{cs}) [17, 18] were numerically compared with respect to the related older theories (PAR_{ds} violating continuity requirements [1–3, 6]. The discrepancies obtained between these different models constitute the subject currently under investigation.

In order to connect the models we are dealing with, to these recent investigations [14–18], it is pointed out that the acronym PAR_{ds} stands, referring to references [6, 8, 17, 18], for parabolic shear deformable theory of laminated plates modelled as equivalent single-layer models (ESL). Differently, the PAR_{cs} model, presented in reference [18], is an improved equivalent single-layer model accounting for the interlaminar continuity of the transversal shear stresses. In this respect, PAR_{cs} preserves the total number of unknowns (avoiding the principal disadvantage of LWMs), in total five, and the related computational effort is independent of the number of layers in the laminate.

Paying particular attention to references [15, 19], it is evident how models violating the interlaminar continuity conditions (say PAR_{ds}) can underestimate/overestimate the global response behaviour with respect to their counterpart models fulfilling the interlaminar continuities (PAR_{cs}). The discrepancies are dependent upon the lamination scheme, as cross- or angle-ply, and can be accentuated whereas different layers exhibit a high rate change in material characteristics, with different transverse shear *moduli*. Similar conclusions were also reported by different authors [20, 21]. However, in spite of the discrepancies that were clearly present, the exactness of the values obtained by different 2-D models cannot be considered a closed question. Indeed, by using the exact results, assessed by the three-dimensional theory of elasticity, it can be shown how the model PAR_{cs}, can give poorer results than its counterpart PAR_{ds} (see also reference [16]). As it can be evidently suggested by graphical representations, the higher order theory accounting for the interlaminar continuity conditions of the transverse shear stress (PAR_{cs}) can introduce a certain "distortion" of the transversal sections than it is done by the corresponding theory violating the interlaminar continuity conditions (PAR_{ds}). The "distortion" can be caused by a real 3-D strong non-linear variation of the in-plane response. As the number of layers increases through the same thickness of the plate a "zig–zag" variation becomes more and more linear and the PAR_{cs} becomes more reliable than the corresponding PAR_{ds} theory.

The question that arises is whether a generalized displacement-based model, violating the continuity of the transverse shear stresses but having higher order terms than the cubic one, would be able to recover an accuracy of the global response in cases of practical importance from an engineering point of view. This question has been taken into account by other researchers in the past [3, 4, 5, 7, 9, 10, 14, 15, 22] showing good results with respect to the previous classical theories. However, such generalizations, apart from the importance given to the normal effect (e.g. references [4, 5, 9]), were never carried out beyond the cubic terms. It is only in the light of the recent developments of higher-speed digital computers that the implementation of such generalized theories is feasible, and, in this respect, they are possibly practicable and up to date. With respect to the question that has been raised, generalized

D2D models, as shown hereafter, are not generally able, to predict satisfactorily relevant exact results except for some cases for which these models predict the global response more accurately than the advanced PAR_{cs} models fulfilling the continuity requirements [23, 24].

In order to encompass the relevant trends in the subject of free vibration studies of laminated plates, an expected more accurate model (M2D) has also been developed in this work. This model differs from the previous one (D2D) by modelling the transverse shear stress as well as the displacement field by using a mixed variational approach. The model M2D is expected to be more accurate than the D2D one because it is able to overcome the deficiency of the discontinuous interlaminar stresses introduced by the constitutive equations and, for which, all the pure displacement-based models (PAR_{ds}, D2D) undergo. There is literature on different proposal concerned with such a mixed approach [25–30], whereas it is believed that the most important step was originated by Reissner's works ranging from references [31] to [32]. The present M2D model is mainly inspired by reference [32]. Such a mixed variational approach was applied by Toledano and Murakami [25, 26] to Reissner's theoretical base for the static analysis of plates. An extension to the dynamic analysis of plates and shells has been recently considered by Carrera [29, 30] that presented the relevant models accounting for the effect of the transverse normal stress usually neglected in 2-D models. Namely, reference [29] considers the mixed approach in the frame of the layer-wise models comparing its results with those of several authors in both ESL and LW models. In addition, reference [30] describes a layer-wise mixed model with an equivalent single-layer model in a unified notation. With respect to the objectives herein pursued it should be of interest to mention that such ESL models in reference [30] are: (i) the classical displacement equivalent single-layer models, where the displacement variables are expressed in Taylor series throughout the thickness of the laminate with unknown variables defined on the middle surface; (ii) mixed equivalent single-layer models, where, if the displacement field is modelled in the framework of ESL-type models, according to reference [25], the transverse stress is modelled in a layer-wise description to properly impose the boundary conditions.

Finally, references [28, 33] which present generalized higher order models are also worth mentioning. Reference [28] presents a generalized nth order beam theory in the frame of geometrical non-linear elasticity and, constitutes, to the best of the author's knowledge, the only generalized mixed higher order theory found in literature, but for beam models and without any particular numerical results. Moreover, reference [33] deals with the theoretical aspects, without any numerical results, encompassing several displacement-based transverse shear and normal deformable plate theories in a generalized one, by a certain vectorial formulation compared to a variational one.

In the scenario described above the present work aims to introduce two different generalized higher order 2-D models for free vibration studies in which laminated plates are involved. These theories are introduced in order to model the displacement field and the transverse shear stress (whenever M2D is considered) throughout the thickness of the laminated by using continuous functions that are able to simultaneously satisfy the boundary conditions at the top and those at the bottom of the laminate besides accounting for the continuity requirements at the interfaces. The particular orthogonal polynomial bases are used to simplify the formulations of the relevant dynamical problems that in its nature is conditioned [23, 27]. Such polynomial bases were in part used in conjunction with Ritz's method [9, 14, 34] in different contexts. The investigation herein conducted is strictly related to those theories neglecting the transverse normal stress (e.g. [1–3, 6, 7, 10, 11, 15–19, 22, 23] and for this reason the same transverse normal stress has been neglected. It should be, however, noted that references [29–30] recently quoted relevant conclusions on this effect from the static and the dynamical points of view.

The M2D model is built by expanding both in-plane displacements and the transverse shear stress by using orthogonal polynomials. Different bases are used for displacement and/or stress fields. The difference between these bases is related to different conditions that the mentioned fields should satisfy at the top and bottom of the laminate. A third different base is used to develop the D2D model. However, it should be stressed that the expansion in both cases, D2D and M2D, is carried out by a linear combination of continuous functions having continuous derivative. In this respect, model M2D should be able to account for the continuity of displacement components (layers perfectly bonded together) and the continuity of transverse shear stress. Nevertheless, the natural discontinuities through the thickness of the laminate [23, 24] cannot be exactly fulfilled. The requirements connected with continuities through the thickness of the laminate can then be considered fulfilled in a weaker form.

Once the theoretical work introducing the governing equations for both models (D2D, M2D) is carried out in a unified notation, several numerical tests are presented to test both models against the 3-D theory of elasticity in cylindrical bending conditions. The details of the 3D model are presented in reference [16] as initially proposed in references [35, 36] and, therefore, they will not be reprocessed here.

Convergence tests compared to the exact results of the elasticity give a benchmark figure with respect to the best values obtainable by the presented generalized ESLnth-type higher order for 2-D models in which the transverse normal stress is neglected.

2. THE GENERALIZED DISPLACEMENT-BASED PLATE THEORY: D2D

Consider a composite laminated plate of uniform thickness h having an axial and transverse length L_x, L_y respectively (Figure 1). The axial, transversal and normal to the middle-surface co-ordinate length parameters are denoted by x, y and z, respectively, whereas U, V and W represent the corresponding displacement components. The plate is made of an arbitrary number, L, of linearly elastic monoclinic layers, the material axes of which are indicated by the lamination angle θ with respect to the x-axis (Figure 1).

In line with the "method of hypotheses" [37], the components of displacements are initially assumed as follows:

$$\begin{aligned} U(x, y, z; t) &= u(x, y; t) - z w_{,x} + \Phi_{1j}(z)\, u_j(x, y; t), \\ V(x, y, z; t) &= v(x, y; t) - z w_{,y} + \Phi_{2j}(z)\, v_j(x, y; t), \\ W(x, y, z; t) &= w(x, y; t), \end{aligned} \tag{1}$$

where the usual convention of repeated indices $j = 1, \ldots, N$ is adopted in place of the relevant summation. Throughout the whole paper only the index j will be adopted under this assumption unless otherwise specified. The displacement field (1) can be considered an extension of the expansions assumed by references [1–3, 6]. The crucial point is connected with a choice of the particular components or the so-called shape functions (Φ_{1j}, Φ_{2j}). This will be tackled in order to satisfy the boundary conditions on the top and bottom of the plate.

From expressions (1) it is clear how the generalized higher order theory is dictated by $(2N + 3)$ displacement components (u, v, $u_1, \ldots, u_N$, $v_l, \ldots, v_N$, w) and, consequently, computational demand is added with respect to $\mathrm{PAR}_{\mathrm{ds}}$ model. The computational effort should be then justifiable in the light of remarkable improvements. As far as the strain displacement equations are concerned, they can be obtained by three-dimensional elasticity

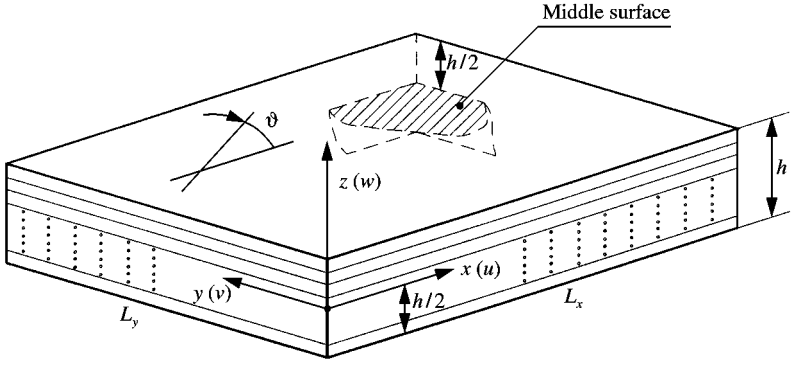

Figure 1. Nomenclature and co-ordinate system of the laminated plate.

as follows [$(\,)' = (\mathrm{d}/\mathrm{d}z)(\,)$]:

$$\varepsilon_x = u_{,x} - zw_{,xx} + \Phi_{1j}u_{j,x}, \quad \varepsilon_y = v_{,y} - zw_{,yy} + \Phi_{2j}v_{j,y}, \quad \varepsilon_z = 0,$$

$$\gamma_{xy} = u_{,y} + v_{,x} - 2zw_{,xy} + \Phi_{1j}u_{j,y} + \Phi_{2j}v_{j,x}, \quad \gamma_{xz} = \Phi'_{1j}u_j, \quad \gamma_{yz} = \Phi'_{2j}v_j, \tag{2}$$

where it is revealed that the shape functions $\Phi_{1j}(z)$ and $\Phi_{2j}(z)$ are still directly responsible for modelling the transverse shear strain through the thickness, h, of the laminate. Hence, under the usual two-dimensional theory of negligible transverse normal stress, the constitutive relationships in the kth monoclinic layer (starting to count from the bottom) are given as follows ($k = 1, 2, \ldots, L$):

$$\begin{bmatrix} \sigma_x^{(k)} \\ \sigma_y^{(k)} \\ \tau_{xy}^{(k)} \end{bmatrix} = \begin{bmatrix} Q_{11}^{(k)} & Q_{12}^{(k)} & Q_{16}^{(k)} \\ Q_{12}^{(k)} & Q_{22}^{(k)} & Q_{26}^{(k)} \\ Q_{16}^{(k)} & Q_{26}^{(k)} & Q_{66}^{(k)} \end{bmatrix} \begin{bmatrix} \varepsilon_x \\ \varepsilon_y \\ \gamma_{xy} \end{bmatrix},$$

$$\begin{bmatrix} \tau_{yz}^{(k)} \\ \tau_{xz}^{(k)} \end{bmatrix} = \begin{bmatrix} Q_{44}^{(k)} & Q_{45}^{(k)} \\ Q_{45}^{(k)} & Q_{55}^{(k)} \end{bmatrix} \begin{bmatrix} \gamma_{yz} \\ \gamma_{xz} \end{bmatrix}, \tag{3}$$

where the appearing reduced stiffness are defined in Whitney [38].

Finally, the governing partial differential equation can be consistently obtained on the basis of Hamilton's principle:

$$\int_{t1}^{t2} (\delta T - \delta \hat{U})\,\mathrm{d}t = 0, \tag{4}$$

where

$$\delta T = \int_{Vol} \rho(\dot{U}\,\delta\dot{U} + \dot{V}\,\delta\dot{V} + \dot{W}\,\delta\dot{W})\,\mathrm{d}\,Vol,$$

$$\delta \hat{U} = \int_{Vol} (\sigma_x\,\delta\varepsilon_x + \sigma_y\,\delta\varepsilon_y + \tau_{xy}\,\delta\gamma_{xy} + \tau_{xz}\,\delta\gamma_{xz} + \tau_{yz}\,\delta\gamma_{yz})\,\mathrm{d}\,Vol. \tag{5}$$

Therefore, applying equation (4) according to equation (1–3), and carrying out the usual integrations (decomposing the volume in surface and thickness) herein not reported for the sake of brevity, the following governing equations are obtained:

$$
\begin{aligned}
&N_{x,x} + N_{xy,y} = \rho_o \ddot{u} - \rho_1 \ddot{w}_{,x} + \rho_o^{1j} \ddot{u}_j,\\
&N_{y,y} + N_{xy,x} = \rho_o \ddot{v} - \rho_1 \ddot{w}_{,y} + \rho_o^{2j} \ddot{v}_j,\\
&M_{x,xx} + M_{y,yy} + 2M_{xy,xy} = \rho_o \ddot{w} - \rho_2 (\ddot{w}_{,xx} + \ddot{w}_{,yy}) + \rho_1 (\ddot{u}_{,x} + \ddot{v}_{,y}) + \rho_1^{1j} \ddot{u}_{j,x} + \rho_1^{2j} \ddot{v}_{j,y},\\
&M_{xi,x} + M_{xy1i,y} - Q_{xi} = \rho_o^{11} \ddot{u} - \rho_1^{11} \ddot{w}_{,x} + \rho_o^{11,1j} \ddot{u}_j,\\
&\cdots\\
&M_{xi,x} + M_{xy1i,y} - Q_{xi} = \rho_o^{1i} \ddot{u} - \rho_1^{1i} \ddot{w}_{,x} + \rho_o^{1i,1j} \ddot{u}_j, \quad i = 1, \ldots, N,\\
&\cdots\\
&M_{xN,x} + M_{xy1N,y} - Q_{xN} = \rho_o^{1N} \ddot{u} - \rho_1^{1N} \ddot{w}_{,x} + \rho_o^{1N,1j} \ddot{u}_j,\\
&M_{y1,y} + M_{xy21,x} - Q_{y1} = \rho_o^{2l} \ddot{v} - \rho_1^{21} \ddot{w}_{,y} + \rho_o^{21,2j} \ddot{v}_j,\\
&\cdots\\
&M_{yi,y} + M_{xy2i,x} - Q_{yi} = \rho_o^{2i} \ddot{v} - \rho_1^{2i} \ddot{w}_{,y} + \rho_o^{2i,2j} \ddot{v}_j, \quad i = 1, \ldots, N,\\
&\cdots\\
&M_{yN,y} + M_{xy2N,x} - Q_{yN} = \rho_o^{2N} \ddot{v} - \rho_1^{2N} \ddot{w}_{,y} + \rho_o^{2N,2j} \ddot{v}_j,
\end{aligned}
\tag{6}
$$

where the resultant generalized stresses and inertia terms are given according to the following equations:

$$
(N_x, N_y, N_{xy}) = \int_{-h/2}^{h/2} (\sigma_x, \sigma_y, \tau_{xy})\, \mathrm{d}z, \quad (M_x, M_y, M_{xy}) = \int_{-h/2}^{h/2} (\sigma_x, \sigma_y, \tau_{xy})\, z\, \mathrm{d}z,
$$

$$
(M_{xi}, M_{yi}, M_{xy1i}, M_{xy2i}) = \int_{-h/2}^{h/2} (\sigma_x \Phi_{1i}, \sigma_y \Phi_{2i}, \tau_{xy} \Phi_{1i}, \tau_{xy} \Phi_{2i})\, \mathrm{d}z. \tag{7}
$$

$$
(Q_{xi}, Q_{yi}) = \int_{-h/2}^{h/2} (\tau_{xz} \Phi'_{1i}, \tau_{yz} \Phi'_{2i})\, \mathrm{d}z.
$$

$$
\rho_k = \int_{-h/2}^{h/2} \rho z^k\, \mathrm{d}z, \quad \rho_o^{lm,np} = \int_{-h/2}^{h/2} \rho \Phi_{lm} \Phi_{np}\, \mathrm{d}z, \tag{8}
$$

$$
\rho_k^{lm} = \int_{-h/2}^{h/2} \rho \Phi_{lm} z^k\, \mathrm{d}z
$$

with the following equations correlating the resultant generalized stresses (7) with the displacement components:

$$
\begin{bmatrix}
N_x \\ N_y \\ N_{xy} \\ M_x \\ M_y \\ M_{xy} \\ M_{x1} \\ \vdots \\ M_{xN} \\ M_{y1} \\ \vdots \\ M_{yN} \\ M_{xy11} \\ \vdots \\ M_{xy1N} \\ M_{xy21} \\ \vdots \\ M_{xy2N}
\end{bmatrix}
=
\begin{bmatrix}
A_{11} & A_{12} & A_{16} & B_{11} & B_{12} & B_{16} & B_{11,11} & \cdots & B_{11,1N} & B_{12,21} & \cdots & B_{12,2N} & B_{16,11} & \cdots & B_{16,1N} & B_{16,21} & \cdots & B_{16,2N} \\
 & A_{22} & A_{26} & B_{12} & B_{22} & B_{26} & B_{12,11} & \cdots & B_{12,1N} & B_{22,21} & \cdots & B_{22,2N} & B_{26,11} & \cdots & B_{26,1N} & B_{26,21} & \cdots & B_{26,2N} \\
 & & A_{66} & B_{16} & B_{26} & B_{66} & B_{16,11} & \cdots & B_{16,1N} & B_{26,21} & \cdots & B_{26,2N} & B_{66,11} & \cdots & B_{66,1N} & B_{66,21} & \cdots & B_{66,2N} \\
 & & & D_{11} & D_{12} & D_{16} & D_{11,11} & \cdots & D_{11,1N} & D_{12,21} & \cdots & D_{12,2N} & D_{16,11} & \cdots & D_{16,1N} & D_{16,21} & \cdots & D_{16,2N} \\
 & & & & D_{22} & D_{26} & D_{12,11} & \cdots & D_{12,1N} & D_{22,21} & \cdots & D_{22,2N} & D_{26,11} & \cdots & D_{26,1N} & D_{26,21} & \cdots & D_{26,2N} \\
 & & & & & D_{66} & D_{16,11} & \cdots & D_{16,1N} & D_{26,21} & \cdots & D_{26,2N} & D_{66,11} & \cdots & D_{66,1N} & D_{66,21} & \cdots & D_{66,2N} \\
 & & & & & & D_{11,11,11} & \cdots & D_{11,11,1N} & D_{12,11,21} & \cdots & D_{12,11,2N} & D_{16,11,11} & \cdots & D_{16,11,1N} & D_{16,21,21} & \cdots & D_{16,21,2N} \\
 & & & & & & & \ddots & \vdots & \vdots & \ddots & \vdots & \vdots & \ddots & \vdots & \vdots & \ddots & \vdots \\
 & & & & & & & & D_{11,1N,1N} & D_{12,1N,21} & \cdots & D_{12,1N,2N} & D_{16,1N,11} & \cdots & D_{16,1N,1N} & D_{16,2N,21} & \cdots & D_{16,2N,2N} \\
 & & & & & & & & & D_{22,21,21} & \cdots & D_{22,21,2N} & D_{26,11,11} & \cdots & D_{26,11,1N} & D_{26,21,21} & \cdots & D_{26,21,2N} \\
 & & & & & & & & & & \ddots & \vdots & \vdots & \ddots & \vdots & \vdots & \ddots & \vdots \\
 & & & & & & & & & & & D_{22,2N,2N} & D_{26,1N,11} & \cdots & D_{26,1N,1N} & D_{26,2N,21} & \cdots & D_{26,2N,2N} \\
 & & & & & & & & & & & & D_{66,11,11} & \cdots & D_{66,11,1N} & D_{66,11,21} & \cdots & D_{66,11,2N} \\
 & & & & & & & & & & & & & \ddots & \vdots & \vdots & \ddots & \vdots \\
 & & & & & & & & & & & & & & D_{66,1N,1N} & D_{66,1N,21} & \cdots & D_{66,1N,2N} \\
 & & & & & & & & & & & & & & & D_{66,21,21} & \cdots & D_{66,21,2N} \\
 & & & & & & & & & & & & & & & & \ddots & \vdots \\
 & & & & & & & & & & & & & & & & & D_{66,2N,2N}
\end{bmatrix}
\begin{bmatrix}
u_{,x} \\ v_{,y} \\ (u_{,y} + v_{,x}) \\ -w_{,xx} \\ -w_{,yy} \\ -2w_{,xy} \\ u_{1,x} \\ \vdots \\ u_{N,x} \\ v_{1,y} \\ \vdots \\ v_{N,y} \\ u_{1,y} \\ \vdots \\ u_{N,y} \\ v_{1,x} \\ \vdots \\ v_{N,x}
\end{bmatrix}, \tag{9}
$$

$$\begin{pmatrix} Q_{y1} \\ \vdots \\ Q_{yN} \\ Q_{x1} \\ \vdots \\ Q_{xN} \end{pmatrix} = \begin{bmatrix} A_{44,21,21} & \cdots & A_{44,21,2N} & A_{45,21,11} & \cdots & A_{45,21,1N} \\ & \ddots & \vdots & \vdots & \ddots & \vdots \\ & & A_{44,2N,2N} & A_{45,2N,11} & \cdots & A_{45,2N,1N} \\ & & & A_{55,11,11} & \cdots & A_{55,11,1N} \\ & sym & & & \ddots & \vdots \\ & & & & & A_{55,1N,1N} \end{bmatrix} \cdot \begin{pmatrix} v_1 \\ \vdots \\ v_N \\ u_1 \\ \vdots \\ u_N \end{pmatrix} \tag{10}$$

with the plate stiffness having the following expressions:

$$A_{ij} = \int_{-h/2}^{h/2} Q_{ij}^{(k)} \, \mathrm{d}z, \quad B_{ij} = \int_{-h/2}^{h/2} Q_{ij}^{(k)} \, z \, \mathrm{d}z, \quad B_{ij,lp} = \int_{-h/2}^{h/2} Q_{ij}^{(k)} \, \Phi_{lp} \, \mathrm{d}z,$$

$$D_{ij} = \int_{-h/2}^{h/2} Q_{ij}^{(k)} \, z^2 \, \mathrm{d}z, \quad D_{ij,lp} = \int_{-h/2}^{h/2} Q_{ij}^{(k)} \, \Phi_{lp} \, z \, \mathrm{d}z, \quad D_{ij,lp,nq} = \int_{-h/2}^{h/2} Q_{ij}^{(k)} \, \Phi_{lp} \Phi_{nq} \, \mathrm{d}z, \tag{11}$$

$$A_{ij,lp,nq} = \int_{-h/2}^{h/2} Q_{ij}^{(k)} \, \Phi'_{lp} \Phi'_{nq} \, \mathrm{d}z.$$

Finally, the consistent boundary conditions along the edges of the plate require the following prescriptions:

along $x = 0, L_x$,

$$N_x = 0 \quad \text{or} \quad u, \quad N_{xy} = 0 \quad \text{or} \quad v, \quad M_{xi} = 0 \quad \text{or} \quad u_i, \quad M_{xy2i} = 0 \quad \text{or} \quad v_i, \quad M_x = 0 \quad \text{or} \quad w_{,x}$$
$$(M_{x,x} + 2M_{xy,y} - \rho_1 \ddot{u} + \rho_2 \ddot{w}_{,x} - \rho_1^{1j} \ddot{u}_j) = 0 \quad \text{or} \quad w. \tag{12}$$

along $y = 0, L_y$,

$$N_y = 0 \quad \text{or} \quad v, \quad N_{xy} = 0 \quad \text{or} \quad u, \quad M_{yi} = 0 \quad \text{or} \quad v_i, \quad M_{xy1i} = 0 \quad \text{or} \quad u_i, \quad M_y = 0 \quad \text{or} \quad w_{,y}$$
$$(M_{y,y} + 2M_{xy,y} - \rho_1 \ddot{v} + \rho_2 \ddot{w}_{,y} - \rho_1^{2j} \ddot{v}_j) = 0 \quad \text{or} \quad w.$$

As far as the expansion is concerned, an appropriate polynomial base should be chosen to satisfy the boundary conditions on the bottom and top of the plate. Namely, combining equations (2, 3):

$$\begin{bmatrix} \tau_{yz}^{(k)} \\ \tau_{xz}^{(k)} \end{bmatrix} = \begin{bmatrix} Q_{44}^{(k)} & Q_{45}^{(k)} \\ Q_{45}^{(k)} & Q_{55}^{(k)} \end{bmatrix} \begin{bmatrix} \Phi'_{2j} & v_j \\ \Phi'_{1j} & u_j \end{bmatrix}. \tag{13}$$

Equation (13) suggests, as a proper choice, an expansion through the z-co-ordinate for which the derivatives of the shape functions are identically 0 at the bottom and top of the plate ($\pm h/2$). Moreover, mathematical reasons suggest to make use of orthogonal polynomials to average functions C_z^0 continuous. The orthogonal polynomials have been symbolically obtained by the Gram–Schmidt orthogonalization process [39] carried out on independent functions having an extremum at $\xi = z/h = \pm 1/2$. The independent functions have been obtained by using the following equations:

$$p(\xi)_0 = 1, \quad \xi = z/h,$$

$$p(\xi)_n = a_1 \xi + a_2 \xi^2 + \xi^3 + \xi^4 + \cdots + \xi^{n-1} + \xi^n, \quad n = 3, \ldots, N,$$

$$a_1 = -\left(\frac{3}{2^2} + \frac{5}{2^4} + \cdots + \frac{n_{odd}}{2^{n_{odd}-1}} \right), \quad a_2 = -\left(\frac{4}{2^3} + \frac{6}{2^5} + \cdots + \frac{n_{even}}{2^{n_{even}-1}} \right), \tag{14}$$

with (n_{odd}, n_{even}) indicating the maximum odd or even number related to the truncation number n. On the basis of equations (14) the Gram–Schmidt process [39] has been symbolically carried out to obtain orthonormal polynomials with zero derivative at $\xi = z/h = \pm 1/2$. Concluding, the ith shape function Φ_i (Φ_{1i} or Φ_{2i}) is assumed to be the ith component belonging to the mentioned set of orthonormal polynomials, the first three of which are shown below as in equation (15).

$$\Phi(\xi)_1 = \sqrt{35/17}(-3\xi + 4\xi^3)$$

$$\Phi(\xi)_2 = \sqrt{525}(-\xi^2 + 2\xi^4 + 7/120),$$

$$\Phi(\xi)_3 = \sqrt{2618/13}(105\xi/136 - 145\xi^3/17 + 18\xi^5); \quad j = 4, \ldots, N. \tag{15}$$

It is worth mentioning that this model contains the previous shear deformable theory PAR_{ds} [6] as a particular case. Indeed, whenever only the first term of equation (15) is retained, within the expansion concerning displacement field (1), the PAR_{ds} higher order theory is evidently obtained. Indeed, the first term in equation (15) corresponds to the cubic shape function adopted in PAR_{ds} [6] or equivalent models. With the aim of keeping the (u_j, v_j) degrees of freedom dimensionless, each term in equation (15) can be used in equation (1) pre-multiplied by thickness h.

3. THE GENERALIZED MIXED-BASED PLATE THEORY: M2D

Still with respect to Figure 1 and a view towards the application of such a mixed approach [32], two independent fields are assumed for both displacement and stress variables. To this end, the components of displacements are initially assumed as reported above in equation (1). As dictated by Reissner's work [32] only a part of the stresses is assumed and, therefore, the transverse shear stress is expanded on a general functional base as reported in equation (16). The normal stress is assumed to be zero.

$$\tau_{yz} = \alpha(z)_j \, \tau(x, y; t)_{yzj},$$

$$\tau_{xz} = \beta(z)_j \, \tau(x, y; t)_{xzj}, \quad -h/2 \leqslant z \leqslant h/2, \tag{16}$$

$$\sigma_z = 0.$$

In equation (16) the convention of repeated indices $j = 1, \ldots, N$ is still adopted in place of relevant summations. It should be interesting to note that a different N could be adopted for displacement and stress and herein they will be indicated by N_u and N_σ respectively. In such circumstances, a double computational demand seems to be correlated with such a mixed model, with respect to the previous D2D theory. However, as hereafter reported, any computational effort is not effectively added relating to the free vibration studies this paper is dealing with.

In accordance with the mixed variational approach [32], the theory should be based on a mixed field of stress and strains. Therefore, half of the stresses, $\boldsymbol{\sigma}_{ou}^{\text{T}} = (\tau_{yz}, \tau_{xz}, \sigma_z)$, are assumed by equation (16), the remaining ones, $\boldsymbol{\sigma}_{in}^{\text{T}} = (\sigma_x, \sigma_y, \tau_{xy})$, are dependent on the strains coming from the classical 3-D constitutive equations (17) with respect to the kth monoclinic layer. The latter dependencies can be conveniently considered

as in equation (17):

$$\left\{\begin{matrix}\sigma_x^k\\ \sigma_y^k\\ \tau_{xy}^k\end{matrix}\right\} = \left[\begin{matrix}C_{11}^k & C_{12}^k & C_{16}^k\\ C_{12}^k & C_{22}^k & C_{26}^k\\ C_{16}^k & C_{26}^k & C_{66}^k\end{matrix}\right]\left[\begin{matrix}0 & 0 & C_{13}^k\\ 0 & 0 & C_{23}^k\\ 0 & 0 & C_{36}^k\end{matrix}\right]\cdot = \left\{\begin{matrix}\varepsilon_x^k\\ \varepsilon_y^k\\ \gamma_{xy}^k\end{matrix}\right\} = \left[\begin{matrix}\mathbf{C}_{126}^k & \mathbf{D}^k\\ \mathbf{D}^{k\mathrm{T}} & \mathbf{C}_{345}^k\end{matrix}\right]\left\{\begin{matrix}\mathbf{e}_{in}\\ \mathbf{e}_{ou}\end{matrix}\right\}.$$
$$\left\{\begin{matrix}\tau_{yz}^k\\ \tau_{xz}^k\\ \sigma_z^k\end{matrix}\right\} \left[\begin{matrix}0 & 0 & 0\\ 0 & 0 & 0\\ C_{13}^k & C_{23}^k & C_{36}^k\end{matrix}\right]\left[\begin{matrix}C_{44}^k & C_{45}^k & 0\\ C_{45}^k & C_{55}^k & 0\\ 0 & 0 & C_{33}^k\end{matrix}\right] \left\{\begin{matrix}\gamma_{yz}^k\\ \gamma_{xz}^k\\ \varepsilon_z^k\end{matrix}\right\} \tag{17}$$

Moreover, by simple algebraic manipulations carried out on the partitioned sub-matrices of equation (17) the following equations can be easily established:

$$\begin{aligned}\boldsymbol{\sigma}_{in} &= (\mathbf{C}_{126}^k - \mathbf{D}^k\,(\mathbf{C}_{345}^k)^{-1}\,\mathbf{D}^{k\mathrm{T}})\,\mathbf{e}_{in} + \mathbf{D}^k\,(\mathbf{C}_{345}^k)^{-1}\,\boldsymbol{\sigma}_{ou},\\ \mathbf{e}_{ou} &= (\mathbf{C}_{345}^k)^{-1}\,\boldsymbol{\sigma}_{ou} - (\mathbf{C}_{345}^k)^{-1}\,\mathbf{D}^{k\mathrm{T}}\,\mathbf{e}_{in}.\end{aligned} \tag{18}$$

The mixed variational equation can then be considered, similar to reference [30], for the dynamic case which is

$$\int_{Vol}[\boldsymbol{\sigma}_{in}^{\mathrm{T}}\,\delta\mathbf{e}_{in}^{(G)} + \boldsymbol{\sigma}_{ou}^{\mathrm{T}}\delta\mathbf{e}_{ou}^{(G)} + \delta\boldsymbol{\sigma}_{ou}^{\mathrm{T}}\,(\mathbf{e}_{ou}^{(G)} - \mathbf{e}_{ou}^{(C)}) + \rho(\ddot{U}\,\delta U + \ddot{V}\,\delta V + \ddot{W}\,\delta W)]\,\mathrm{d}\,Vol = 0, \tag{19}$$

where the subscript T stands for the transpose operator. The superscripts in parentheses (G, C) state that the relevant out-of-plane strains ($\mathbf{e}_{ou}$) should be introduced, into equation (19), by using geometric equations (2) and constitutive equations (18) respectively. Conversely, the in-plane strains are related to the displacement always by kinematics equations (2). Finally, in-plane ($\boldsymbol{\sigma}_{in}$) and out-of-plane ($\boldsymbol{\sigma}_{ou}$) stresses should be assessed by using constitutive equations (18) and assumed field (16) respectively.

Therefore, applying equation (19) according to equations (1–2, 16, 18), and carrying out the usual integrations, herein not reported for the sake of brevity, the governing equations are obtained identically to equations (6) and (7), apart from a few localized changes. As far as these changes are concerned, firstly, equation (6) contain $2N_\sigma$ more *algebraic* equations. Secondly, the generalized global transverse stresses (Q_{xi}, Q_{yi}) are not defined as in equation (7) but, upon the assumed transverse stress field (16). In conclusion, a localized part of the previously D2D model results as changed by the mixed variational approach in the part strictly depending on the shear stress contribution. The following equations clarify the mentioned terms consistently obtained through equation (19).

The mentioned *albegraic* equations, that must be added to equation (6), are conveniently reported as

$$\bar{\Gamma}_{ij}\tau_{yzj} + \underline{\Gamma}_{ij}\tau_{xzj} = \Xi_{2ik}\,v_k, \quad \underline{\underline{\Gamma}}_{ij}\tau_{yzj} + \bar{\bar{\Gamma}}_{ij}\tau_{xzj} = \Xi_{1ik}\,u_k \quad i,j,k = 1,\ldots,N_\sigma, N_\sigma, N_u) \tag{20}$$

whereas any single equation in equation (20) is obtained by fixing the i- with (j,k)-index indicating relevant summations on the convention of repeated indices in any single ith equation. The relevant coefficients of the *algebraic* equation in equation (20) correspond to the following terms:

$$\begin{aligned}\bar{\Gamma}_{ij} &= \int_{-h/2}^{h/2} E_{11}^k\,\alpha(z)_i\,\alpha(z)_j\,\mathrm{d}z, \quad \bar{\bar{\Gamma}}_{ij} = \int_{-h/2}^{h/2} E_{22}^k\,\beta(z)_i\,\beta(z)_j\,\mathrm{d}z, \quad \Xi_{2ik} = \int_{-h/2}^{h/2}\alpha(z)_i\,\Phi(z)'_{2k}\,\mathrm{d}z,\\ \underline{\Gamma}_{ij} &= \int_{-h/2}^{h/2} E_{12}^k\,\alpha(z)_i\,\beta(z)_j\,\mathrm{d}z, \quad \underline{\underline{\Gamma}}_{ij} = \int_{-h/2}^{h/2} E_{12}^k\,\beta(z)_i\,\alpha(z)_j\,\mathrm{d}z, \quad \Xi_{1ik} = \int_{-h/2}^{h/2}\beta(z)_i\,\Phi(z)'_{1k}\,\mathrm{d}z,\end{aligned} \tag{21}$$

whereas the compliance coefficients E^k_{11}, E^k_{12}, E^k_{22}, are respectively $(\mathbf{C}^k_{345})^{-1}_{11}$, $(\mathbf{C}^k_{345})^{-1}_{12}$, $(\mathbf{C}^k_{345})^{-1}_{22}$. Moreover, from the fourth equation to $2N$ (in the mixed models say $2N_u$) in equation (6), the equations should be substituted by the following ones:

$$\begin{aligned} M_{xi,x} + M_{xy1i,y} - Q_{xij} &= \rho_o^{1i}\ddot{u} - \rho_1^{1i}\ddot{w}_{,x} + \rho_o^{1i,1k}\ddot{u}_k,i, \quad j,k = 1, \ldots, N_u, N_\sigma, N_u, \\ M_{yi,y} + M_{xy2i,y} - Q_{yij} &= \rho_o^{2i}\ddot{v} - \rho_1^{2i}\ddot{w}_{,y} + \rho_o^{2i,2k}\ddot{v}_k,i, \quad j,k = 1, \ldots, N_u, N_\sigma, N_u \end{aligned} \tag{22}$$

where the same convention of equations (20) is assumed for (i, j, k) and the generalized global transverse stresses in equation (22) can be obtained by the following equations:

$$(Q_{xij}, Q_{yij}) = \int_{-h/2}^{h/2} (\beta(z)_j \tau_{xzj} \Phi'_{1i}, \alpha(z)_j \tau_{yzj} \Phi'_{2i})\, \mathrm{d}z. \tag{23}$$

At this stage it should be of interest to note how the *algebraic* equations (20) correspond to a *linear system of algebraic equations* and, for this reason, the transverse shear stresses components (τ_{yzj}, τ_{xzj}) can be easily expressed as a function of the displacement components (v_k, u_k). The operation consists in solving a $(2N_\sigma \times 2N_\sigma)$ system of linear equations once the functional base, expanding the shear transverse stress (16), is chosen beforehand.

Algebraic and symbolical manipulations can assist to propose a formulation in a more suitable form than equations (20–23) gaining a more clear presentation of M2D with respect to model D2D. In more detail, bringing together equations (20, 21, 23) it is possible to rewrite equations (22) exactly as they are expressed in equation (6), whereas, the global transverse shear stresses (Q_{xi}, Q_{yi}) should be expressed, differently as done in equation (10), as reported in equation (24):

$$\begin{Bmatrix} Q_{y1} \\ \vdots \\ Q_{yN_u} \\ Q_{x1} \\ \vdots \\ Q_{xN_u} \end{Bmatrix} = \begin{bmatrix} \boldsymbol{\alpha}^{\mathrm{T}} & 0 \\ 0 & \boldsymbol{\beta}^{\mathrm{T}} \end{bmatrix} \begin{bmatrix} \mathbf{H}_{11} & \mathbf{H}_{12} \\ \mathbf{H}_{12}^{\mathrm{T}} & \mathbf{H}_{22} \end{bmatrix} \begin{bmatrix} \boldsymbol{\alpha} & 0 \\ 0 & \boldsymbol{\beta} \end{bmatrix} \begin{Bmatrix} v_1 \\ \vdots \\ v_{N_u} \\ u_1 \\ \vdots \\ u_{N_u} \end{Bmatrix}, \tag{24}$$

where, with respect to notations in equations (20, 21), the sub-matrices in equation (24) have the following expressions:

$$\boldsymbol{\alpha} = \int_{-h/2}^{h/2} \begin{bmatrix} \alpha_1 \Phi'_{21} & \cdots & \alpha_1 \Phi'_{2N_u} \\ \vdots & \vdots & \vdots \\ \alpha_{N_\sigma} \Phi'_{21} & \cdots & \alpha_{N_\sigma} \Phi'_{2N_u} \end{bmatrix}, \quad \boldsymbol{\beta} = \int_{-h/2}^{h/2} \begin{bmatrix} \beta_1 \Phi'_{11} & \cdots & \beta_1 \Phi'_{1N_u} \\ \vdots & \vdots & \vdots \\ \beta_{N_\sigma} \Phi'_{11} & \cdots & \beta_{N_\sigma} \Phi'_{1N_u} \end{bmatrix},$$

$$\begin{bmatrix} \mathbf{H}_{11} & \mathbf{H}_{12} \\ \mathbf{H}_{12}^{\mathrm{T}} & \mathbf{H}_{22} \end{bmatrix} = \begin{bmatrix} \bar{\bar{\mathbf{\Gamma}}} & \underline{\bar{\mathbf{\Gamma}}} \\ \bar{\underline{\mathbf{\Gamma}}} & \underline{\underline{\mathbf{\Gamma}}} \end{bmatrix}^{-1}. \tag{25}$$

In conclusion, the M2D model can be presented with the same governing equations of the D2D model, i.e. the same equation (6), the same generalized resultant stresses (7) except for (Q_{xi}, Q_{yi}), the same inertial terms (8), and the same global constitutive equations (9). However, the M2D model should consider equation (24) in place of equation (10). Finally, it is pointed out that during all subsequent observations N_u has been considered equal to N_σ and for this indicated in the abbreviated form as N.

As far as the expansions are concerned, appropriate functional bases should be chosen to satisfy the boundary conditions on the bottom and top of the plate. In particular, the

transverse shear stresses should always fulfill the conditions to be zero at the bottom and top of the multilayered plate: $\tau(z/h = \pm 1/2)_{xz} = \tau(z/h = \pm 1/2)_{yz} = 0$. For the numerical test herein presented the functional base in equation (16) is constituted by a set of orthonormal polynomials the first three of which are

$$\alpha(\xi)_1 = \beta(\xi)_1 = \sqrt{30}(\xi^2 - 1/4), \qquad \alpha(\xi)_2 = \beta(\xi)_2 = \sqrt{210}(2\xi^3 - \xi/2),$$
$$\alpha(\xi)_3 = \beta(\xi)_3 = \sqrt{10}(42\xi^4 - 12\xi^3 + 3/8), \quad j = 4, \ldots, N. \tag{26}$$

They can be recursively obtained successfully by a known equation which was used for the first time by Bath [34] to study the free vibration of plates on the basis of the Ritz method. A normalization processes can assist to make the norm unitary. Each function in the set (26) fulfils the condition to be zero at $\xi = z/h = \pm 1/2$, and for this reason, the same set has been used elsewhere [19] to model geometric "SS" boundary conditions in vibration studies of plates. This choice is then retained appropriate to model the transverse shear stress through the section of the laminate.

The expansion used to model the in-plane components of the displacement field (1) into the M2D model is now considered as a beam completely free (say 'FF') through the z-co-ordinate. Indeed, considering the transverse shear stress is modelled independently of equations (16), any possible displacement field should be permitted and the relevant functional base should not depend on any constraints at the ends. For this reason the functional base in equation (1) is constituted now by a complete set of orthonormal polynomials of which the first three are:

$$\Phi(\xi)_1 = \sqrt{3}(2\xi), \qquad \Phi(\xi)_2 = \sqrt{5}(6\xi^2 - 1/2), \qquad \Phi(\xi)_3 = \sqrt{7}(20\xi^3 - 3\xi), \qquad j = 4, \ldots, N \tag{27}$$

with the remaining ones being recursively obtained as previously indicated in case of the set of equations (26). It is pointed out here that set (27) does not constitute a complete set due to the absence of the constant term. However, the constant term was not accounted for because of the presence of u and v in equation (1).

With the aim of keeping the (u_j, v_j) degrees of freedom dimensionless each term in equation (27) can be used in equation (1) but, pre-multiplied by thickness h. Conversely, equation (26) can be considered as it is presented.

4. NUMERICAL EXAMPLES AND DISCUSSION ON CYLINDRICAL BENDING CASE

In order to test the effectiveness of both proposed models the relevant dynamical equations for certain simply supported plates in cylindrical bending conditions have been considered [40]. The choice was dictated by the possibility of obtaining exact solutions for any kind of lamination angle and stacking sequence in 3-D analysis [40]. Namely, the following "simply supported" boundary and "cylindrical bending" conditions are assumed

$$(u, v, w, u_i, v_i) = f(x, z; t), \tag{28}$$

$$w(0, y) = 0, \qquad w(L_x, y) = 0,$$
$$N_x(0, y) = N_{xy}(0, y) = 0, \qquad N_x(L_x, y) = N_{xy}(L_x, y) = 0,$$
$$M_x(0, y) = M_{xi}(0, y) = M_{xy2i}(0, y) = 0,$$
$$M_x(L_x, y) = M_{x1}(L_x, y) = M_{xy2_i}(L_x, y) = 0, \tag{29}$$

where, by taking into account equations (12), the boundary conditions (29) would correspond to the three-dimensional case [40] having w, σ_x and τ_{xy} nullified at $x = (0, Lx)$. In this work, no details of the 3-D model have been reported because the model has been presented in reference [16]. However, in this paper, the same numerical code was used to obtain a 3-D base for comparison purposes. As far as the D2D and M2D models are concerned the following generalized displacement field is used:

$$(u, v, u_i, v_i) = A^{(u,\, v,\, ui,\, vi)} \cos\left(\frac{n\pi x}{L_x}\right) \cos(\omega t),$$

$$w = A^{(w)} \sin\left(\frac{n\pi x}{L_x}\right) \cos(\omega t), \quad i = 1, \ldots, N, \tag{30}$$

in order to get, by substitution of equation (30) into equation (6), the following exact generalized eigenvalue problem:

$$(\mathbf{K} - \omega^2 \mathbf{M})\mathbf{A} = \mathbf{0} \tag{31}$$

with $\mathbf{A} = (A^{(u)}, A^{(v)}, A^{(w)}, A^{(ul)}, \ldots, A^{(uN)}, A^{(vl)}, \ldots, A^{(vN)})^{\mathrm{T}}$.

After implementing the solution of the generalized eigenvalue problem (31), six numerical tables were produced to test the effectiveness of the proposed models. To this end the following material properties were considered for all subsequent numerical tables:

$$E_1 = 25E_2 = 25E_3, \quad G_{12} = G_{13} = 0{\cdot}5E_2, \quad G_{23} = 0{\cdot}2E_2, \quad v_{12} = v_{13} = v_{23} = 0{\cdot}25, \tag{32}$$

to evaluate the frequency parameter as given by

$$\omega^* = \omega h \sqrt{\frac{\rho}{G_{12}}}. \tag{33}$$

Hence, referring to Table 1, for any fixed value of N, shown in the first column, six columns report the convergence performance of D2D with respect to an increasing number of layers in the same thickness h. Namely, the first frequency parameter is listed when the wave number n is fixed to be 1. In order to check any possible different behaviour, cross- and angle ply, symmetric and antisymmetric laminates have been analyzed. Moreover, in Table 1, each column reporting the frequency parameter is presented in conjunction with the relevant percentage error with respect to the 3-D result. This percentage error is given by

$$e\% = \frac{(\omega^* - \omega^*_{3-D})}{\omega^*_{3-D}} \times 100 \tag{34}$$

to point out that a negative value stands as an underestimation of the relevant result. Conversely, a positive evaluation of $e\%$ states an overestimation of the frequency.

Hence, based on the described arrangement, Table 1 compares four different models, including the presented D2D one, against the $\mathrm{PAR_{ds}}$ [6, 14], $\mathrm{PAR_{cs}}$ [16–18] and the exact 3-D.

The first observation that can be made, concerns the behaviour of the D2D model with respect to its origin ($\mathrm{PAR_{ds}}$). As it was mentioned in section 2 the D2D model is exactly equivalent to $\mathrm{PAR_{ds}}$ when only one term of expansion (15) is retained (say $\mathrm{D2D_1}$). Indeed, Table 1, unaware of the lamination scheme and layers arrangement, lists the frequency parameter, corresponding to $N = 1$, coincident with respective frequencies of $\mathrm{PAR_{ds}}$.

TABLE 1

First frequency parameters, ω^*, for different numbers of expansion terms and different models: 3-*D*, *D2D*, PAR_{ds}, PAR_{cs}; ($h/L_x = 0{\cdot}1$; $n = 1$)

	$[0/90^\circ]$	*e*%	$[0/90/0^\circ]$	*e*%	$[0/90/0/90^\circ]$	*e*%	$[(0/90)_2 0^\circ]$	*e*%	$[0/90^\circ]_6$	*e*%	$[(0/90)_3 0^\circ{}_1]_5$	*e*%
PAR_{cs}	0·0838082	2·59	0·146384	0·09	0·112403	2·69	0·140347	0·33	0·119717	0·29	0·129924	0·13
PAR_{ds}	0·0823808	0·84	0·151077	3·30	0·115672	5·67	0·145701	4·15	0·123267	3·27	0·134168	3·40
D2D, *N*												
1	0·0823808	0·84	0·151077	3·30	0·115672	5·67	0·145701	4·15	0·123267	3·27	0·134168	3.40
2	0·0818501	0·19	0·151077	3·30	0·112590	2·86	0·145701	4·15	0·123063	3·10	0·134168	3·40
3	0·0816917	0·00	0·148925	1·83	0·111888	2·22	0·145142	3·75	0·123062	3·10	0·134055	3·31
4	0·0816912	0·00	0·148925	1·83	0·110910	1·32	0·145142	3·75	0·122983	3·03	0·134055	3·31
5	0·0816598	− 0·04	0·147621	0·94	0·110865	1·28	0·142928	2·17	0·122982	3·03	0·134014	3·28
6	0·0816594	− 0·04	0·147621	0·94	0·110335	0·80	0·142928	2·17	0·122947	3·00	0·134014	3·28
7	0·0816467	− 0·06	0·147297	0·72	0·110268	0·74	0·141136	0·89	0·122930	2·98	0·134013	3·28
8	0·0816460	− 0·06	0·147297	0·72	0·110153	0·63	0·141136	0·89	0·122924	2·98	0·134013	3·28
3-D	0·0816952	—	0·146248	—	0·109461	—	0·139891	—	0·119368	—	0·129758	—
	$[45/-45^\circ]$	*e*%	$[45/-45/45^\circ]$	*e*%	$[(45/-45^\circ)_2]$	*e*%	$[(45/-45)_2/45^\circ]$	*e*%	$[45/-45^\circ]_6$	*e*%	$[(45/-45)_3/45^\circ{}_1]$	*e*%
PAR_{cs}	0·0663629	1·11	0·0911503	0·04	0·0895849	1·42	0·0944397	0·35	0·0954749	0·13	0·0959541	0·05
PAR_{ds}	0·0658395	0·31	0·0929594	2·03	0·0912185	3·27	0·0964630	2·50	0·0972497	1·99	0·0977788	1·95
D2D, *N*												
1	0·0658395	0·31	0·0929594	2·03	0·0912185	3·27	0·0964630	2·50	0·0972497	1·99	0·0977788	1·95
2	0·0657384	0·16	0·0929594	2·03	0·0899278	1·81	0·0964630	2·50	0·0971667	1·91	0·0977788	1·95
3	0·0656663	0·05	0·0921017	1·08	0·0896170	1·46	0·0960575	2·07	0·0971667	1·91	0·0977411	1·91
4	0·0656657	0·05	0·0921017	1·08	0·0890792	0·85	0·0960575	2·07	0·0971349	1·87	0·0977411	1·91
5	0·0656495	0·02	0·0916134	0·55	0·0890560	0·82	0·0952327	1·19	0·0971347	1·87	0·0977219	1·89
6	0·0656482	0·02	0·0916134	0·55	0·0887633	0·49	0·0952327	1·19	0·0971206	1·86	0·0977219	1·89
7	0·0656414	0·01	0·0914918	0·42	0·0887356	0·46	0·0945997	0·52	0·0971138	1·85	0·0977142	1·89
8	0·0656402	0·01	0·0914918	0·42	0·0886749	0·39	0·0945997	0·52	0·0971103	1·85	0·0977142	1·89
3-D	0·0656341	—	0·0911137	—	0·0883295	—	0·0941086	—	0·0953487	—	0·0959047	—

Moreover, it is interesting to notice the monotonic convergence of the frequency parameter from the less approximated value of PAR_{ds} to the exact 3-D frequency. In particular, when a couple of antisymmetric layers are considered ([0/90°] and [45/ − 45°]), three terms into the expansion (15) are sufficient to get the 3-D result with three or four significant digits (that means an extreme reliability from an engineering point of view). However, the reduction of the performances of this model cannot be ignored when layers increase. Indeed, four layers are sufficient to reduce the good behaviour of the D2D shown in the case of two layers. In general, by observing the results shown in Table 1, it can be concluded that firstly, the D2D model does not have an excellent behaviour when many layers are considered to constitute the laminate and secondly, its behaviour is layout dependent. Indeed, the discrepancies, fixing for example $N = 5$, increase with the number of layers in both angle- and cross-ply laminates. Moreover, it could be of interest to note that the better behaviour of PAR_{ds} appears to be even better in the case of two layers than PAR_{cs}, but, by increasing the number of layers, the latter PAR_{cs} behaves conversely better than PAR_{ds} besides presenting minor discrepancies with respect to any fixed N for the D2D model after considering the case of four layers.

It could be of interest to note that in the case of symmetric laminates (fourth, eighth and 12th columns) the convergence is conditioned by only the odd terms of expansion (15). It should evidently be related to the particular in-plane distribution of displacements requiring odd functions through the thickness of the laminate. Table 2 is built on the same arrangement as Table 1 but, relating its comparisons to the M2D model. There is no doubt that generally the M2D behaves better than the D2D model. In particular, it is worth mentioning that the uniform performance of this model stands almost independent of the number of layers. In particular, when $N = 2$ terms are added in expansions (26, 27) just a couple of cases present a discrepancy beyond 1% (1·65 and 1·33% for [0°/90°/0°] and $[(0°/90°)_2\ 0°]$ respectively). Moreover, in the majority of the cases with $N = 2$, the M2D model behaves better than PAR_{cs}. It would not comes as a surprise comparing the results to the computational effort involved. Indeed, two terms mean a plates theory based on 7 d.o.f.s for displacements and consequently more cumbersome with respect to 5 d.o.f.s related to the PAR_{cs}. However, the possibility of modeling the transverse shear stress by continuous functions to average the real trend besides keeping low the complexity of the model with an increasing number of layers, remains interesting with respect to an analytical model that is able to get reliable natural frequencies as shown in Table 2. Also, in Table 2 the convergence, generally from below with a modulated oscillation, seems to be affected only by odd terms in case of symmetrical stacking sequences.

Tables 3, has been reported for a two-fold objective. It was considered to give evidence of the possible improvement that such a generalized theory can give for isotropic plates where interfaces are absent. Moreover, this table goes to test the discrepancy of both the 2-D models presented herein besides testing their effectiveness. As far as the first objective is concerned it is evident that retaining a number of terms equal to or beyond three, in the relevant expansions, there is absolutely no difference between the M2D and the D2D models. In this situation, the displacement-based theory (D2D) behaves equivalently to the mixed-based theory (M2D). This could be expected since both models are able to satisfy the lateral boundary conditions and the continuity requirements through the thickness of the laminate. However, Table 3 clarifies that such generalized theories can be only computationally demanding, without any effective improvement, if they are not properly used. Namely, as far as the discrepancies are concerned, a monotonic increase occurs since -0.1 to -1.0% against an increasing wave number. In this respect, it should be of interest to known that by graphically displaying the relevant mode shapes, herein not reported, the

TABLE 2

First frequency parameters, ω^*, for different numbers of expansion terms and different models: 3-*D*, *M2D*, PAR_{ds}, PAR_{cs}; ($h/L_x = 0{\cdot}1$; $n = 1$)

	[0/90°]	*e*%	[0/90/0°]	*e*%	[0/90/0/90°]	*e*%	$[(0/90)_2 0°]$	*e*%	$[0/90°]_6$	*e*%	$[(0/90)_3 0°_1]_5$	*e*%
PAR_{cs}	0·0838082	2·59	0·146384	0·09	0·112403	2·69	0·140347	0·33	0·119717	0·29	0·129924	0·13
PAR_{ds}	0·0823808	0·84	0·151077	3·30	0·115672	5·67	0·145701	4·15	0·123267	3·27	0·134168	3·40
M2D, *N*												
1	0·0806500	− 1·28	0·143837	− 1·65	0·113288	3·50	0·138037	− 1·33	0·119802	0·36	0·128569	− 0·92
2	0·0809977	− 0·85	0·143837	− 1·65	0·110066	0·55	0·138037	− 1·33	0·119436	0·06	0·128569	− 0·92
3	0·0817015	0·01	0·145844	− 0·28	0·109150	− 0·28	0·139901	0·01	0·119372	0·00	0·129739	− 0·01
4	0·0816482	− 0·06	0·145844	− 0·28	0·108963	− 0·46	0·139901	0·01	0·119401	0·03	0·129739	− 0·01
5	0·0816093	− 0·11	0·146142	− 0·07	0·108836	− 0·57	0·139381	− 0·36	0·119399	0·03	0·129780	0·02
6	0·0816170	− 0·10	0·146142	− 0·07	0·109205	− 0·23	0·139381	− 0·36	0·119437	0·06	0·129780	0·02
7	0·0816104	− 0·10	0·146210	− 0·03	0·109239	− 0·20	0·139652	− 0·17	0·119437	0·06	0·129808	0·04
8	0·0816138	− 0·10	0·146210	− 0·03	0·109406	− 0·05	0·139652	− 0·17	0·119412	0·04	0·129808	0·04
9	0·0816118	− 0·10	0·146209	− 0·03	0·109405	− 0·05	0·139857	− 0·02	0·119412	0·04	0·129763	0·00
10	0·0816134	− 0·10	0·146209	− 0·03	0·109419	− 0·04	0·139857	− 0·02	0·119340	− 0·02	0·129763	0·00
11	0·0816126	− 0·10	0·146203	− 0·03	0·109414	− 0·04	0·139862	− 0·02	0·119337	− 0·03	0·129748	− 0·01
3-D	0·0816952	—	0·146248	—	0·109461	—	0·139891	—	0·119368	—	0·129758	—
	[45/ − 45°]	*e*%	[45/ − 45/45°]	*e*%	$[(45/-45°)_2]$	*e*%	$[(45/-45)_2/45°]$	*e*%	$[45/-45°]_6$	*e*%	$[(45/-45)_3/45°_1]$	*e*%
PAR_{cs}	0·0663629	1·11	0·0911503	0·04	0·0895849	1·42	0·0944397	0·35	0·0954749	0·13	0·0959541	0·05
PAR_{ds}	0·0658395	0·31	0·0929594	2·03	0·0912185	3·27	0·0964630	2·50	0·0972497	1·99	0·0977788	1·95
D2D, *N*												
1	0·0650055	− 0.96	0.0903783	− 0.81	0.0900247	1.92	0.0941281	0.02	0.0955344	0.19	0.0958849	− 0.02
2	0·0653133	− 0·49	0·0903783	− 0·81	0·0886327	0·34	0·0941281	0·02	0·0953718	0·02	0·0958849	− 0·02
3	0·0656297	− 0·01	0·0909154	− 0·22	0·0882111	− 0·13	0·0941504	0·04	0·0953356	− 0·01	0·0958935	− 0·01
4	0·0656277	− 0·01	0·0909154	− 0·22	0·0880816	− 0·28	0·0941504	0·04	0·0953495	0·00	0·0958935	− 0·01
5	0·0656125	− 0·03	0·0910464	− 0·07	0·0880258	− 0·34	0·0938425	− 0·28	0·0953490	0·00	0·0959056	0·00
6	0·0656180	− 0·02	0·0910464	− 0·07	0·0881969	− 0·15	0·0938425	− 0·28	0·0953646	0·02	0·0959056	0·00
7	0·0656153	− 0·03	0·0910817	− 0·04	0·0882121	− 0·13	0·0939627	− 0·15	0·0953643	0·02	0·0959152	0·01
8	0·0656173	− 0·03	0·0910817	− 0·04	0·0882933	− 0·04	0·0939627	− 0·15	0·0953534	0·00	0·0959152	0·01
9	0·0656165	− 0·03	0·0910803	− 0·04	0·0882947	− 0·04	0·0940689	− 0·04	0·0953535	0·00	0·0958949	− 0·01
10	0·0656174	− 0·03	0·0910803	− 0·04	0·0883019	− 0·03	0·0940689	− 0·04	0·0953211	− 0·03	0·0958949	− 0·01
11	0·0656171	− 0·03	0·0910756	− 0·04	0·0883003	− 0·03	0·0940783	− 0·03	0·0953201	− 0·03	0·0958829	− 0·02
3-D	0·0656341	—	0·0911137	—	0·0883295	—	0·0941086	—	0·0953487	—	0·0959047	—

TABLE 3

First frequency parameters, ω^*, for isotropic plates; $h/L_x = 0{\cdot}1$; $\nu = 0{\cdot}3$

	D2D, N							
n	1	3	5	7	PAR	3-D	$e\%$D2D$_7$	$e\%$ PAR
1	0·0473103	0·0473103	0·0473103	0·0473103	0·0473103	0·0473422	− 0·1	− 0·1
2	0·180237	0·180237	0·180237	0·180237	0·180237	0·180672	− 0·2	− 0·2
3	0·378281	0·378279	0·378279	0·378279	0·378281	0·380024	− 0·5	− 0·5
4	0·620463	0·620447	0·620447	0·620447	0·620463	0·624669	− 0·7	− 0·7
5	0·890825	0·890757	0·890757	0·890757	0·890825	0·898528	− 0·9	− 0·9
6	1·17876	1·17855	1·17855	1·17855	1·17876	1·19064	− 1·0	− 1·0
	M2D, N							
n	1	3	5	7	PAR	3-D	$e\%$M2D$_7$	$e\%$ PAR
1	0·0473100	0·0473103	0·0473103	0·0473103	0·0473103	0·0473422	− 0·1	− 0·1
2	0·180226	0·180237	0·180237	0·180237	0·180237	0·180672	− 0·2	− 0·2
3	0·378182	0·378279	0·378279	0·378279	0·378281	0·380024	− 0·5	− 0·5
4	0·620047	0·620447	0·620447	0·620447	0·620463	0·624669	− 0·7	− 0·7
5	0·889649	0·890757	0·890757	0·890757	0·890825	0·898528	− 0·9	− 0·9
6	1·17613	1·17855	1·17855	1·17855	1·17876	1·19064	− 1·0	− 1·0

increasing discrepancy was provided together with the increasing inability of both models (M2D, D2D) to deal with normal effects.

Tables 4 and 5 compare the results obtainable through the D2D and the M2D models for higher frequencies for the worst case presented in Tables 1 and 2. In this respect, Table 4 lists the first natural frequencies for each fixed n, but Table 5 lists an increasing number of frequencies with $n = 1$. As clearly shown in both tables, the M2D model shows a good behaviour when compared to the 3-D results also in the case of higher frequencies. An exception is provided with the sixth mode (Table 5) where a large discrepancy, even in the M2D model, is present (7·6%). However, it should be considered that in that case we are dealing with extremely high frequencies, for which the 3-D w-part of the displacement field was checked to be comparable with the inplane components. PAR_{ds} and PAR_{cs} in such cases are not evidently able to provide such frequencies for the natural limitation of the d.o.f. (five) used in the formulation.

In order to conclude the numerical test and comparisons, Table 6 is presented to evaluate the behaviour of both models when the thickness approaches zero starting from very thick plates ($L_x/h = 2{\cdot}5$) to extremely thin ones ($L_x/h = 500$). As is evident, both two-dimensional models get closer to the 3-D results proving their sensitivity with respect to the physics of the problem (continuity requirements) that indeed becomes immaterial for very thin plates. In any case the M2D model shows the best behaviour whenever compared to the 3-D exact model.

Finally, a graphical representation of the mode shapes (or eigenfunctions) is considered helpful to complete the investigation herein reported. In this respect, Figures 2–6 are displayed, after scaling the first mode shape evaluated by the eigen problem (31), so that the mode shapes in the z direction [see equation (1)] approximately matches the 3-D one at a fixed x-co-ordinate.

TABLE 4

First frequency parameters, ω^*, for orthotropic plates; [0/90/0/90°]; ($h/L_x = 0{\cdot}1$)

	D2D, N							
n	1	3	5	7	PAR_{ds}	3-D	e%D2D$_7$	e% PAR_{ds}
1	0·115672	0·111888	0·110865	0·110268	0·115672	0·109461	0·7	5·7
2	0·352370	0·328915	0·324061	0·321023	0·352370	0·316561	1·4	11·3
3	0·612065	0·564253	0·557127	0·551860	0·612065	0·542971	1·6	12·7
4	0·875924	0·806547	0·799598	0·792924	0·875924	0·779708	1·7	12·3
5	1·14445	1·05553	1·04977	1·04218	1·14445	1·02465	1·7	11·7
6	1·42055	1·31082	1·30586	1·29749	1·42055	1·27545	1·7	11·4
	M2D, N							
n	1	3	5	7	PAR_{cs}	3-D	e%M2D$_7$	e% PAR_{cs}
1	0·113288	0.109150	0.108836	0.109239	0·112403	0·109461	− 0·2	2·7
2	0·335410	0·311781	0·312974	0·315550	0·332740	0·316561	− 0·3	5·1
3	0·570510	0·525477	0·535635	0·541454	0·575222	0·542971	− 0·3	5·9
4	0·802076	0·742103	0·768963	0·778136	0·831635	0·779708	− 0·2	6·7
5	1·02967	0·96240	1·01124	1·02333	1·10678	1·02465	− 0·1	8·0
6	1·25443	1·18663	1·26019	1·27461	1·40561	1·27545	− 0·1	10·2

TABLE 5

Frequency parameters, ω^*, for orthotropic plates; [0/90/0/90°]; ($h/L_x = 0{\cdot}1$; $n = 1$)

	D2D, N							
No	1	3	5	7	PAR_{ds}	3-D	e%D2D$_7$	e% PAR_{ds}
1	0·115672	0·111888	0·110865	0·110268	0·115672	0·109461	0·7	5·7
2	0·314159	0·314159	0·314159	0·314159	0·314159	0·314159	0·0	0·0
3	1·56827	1·55582	1·54683	1·54388	1·56827	1·53891	0·3	1·9
4	2·64884	2·63821	2·50984	2·43944	2·64884	2·38107	2·5	11·2
5	3·10585	3·09678	2·98629	2·92172	3·10585	2·86911	1·8	8·3
6	—	5·15130†	5·13362†	5·02041†	—	4·55831	10·1	—
	M2D, N							
No	1	3	5	7	PAR_{cs}	3-D	e%M2D$_7$	e% PAR_{cs}
1	0·113288	0·109150	0·108836	0·109239	0·112403	0·109461	− 0·2	2·7
2	0·314159	0·314159	0·314159	0·314159	0·314159	0·314159	0·0	0·0
3	1·54805	1·55199	1·54249	1·53967	1·56071	1·53891	0·1	1·4
4	2·41101	2·39392	2·38652	2·38205	2·64884	2·38107	0·0	0·1
5	2·91497	2·89007	2·89426	2·87932	2·89643	2·86911	0·4	1·0
6	—	5·00755†	4·92504†	4·90682†	—	4·55831	7·6	—

† Appearing as the seventh mode compared to the sixth one of the 3-D model.

In Figure 2, the PAR_{ds} and the D2D solutions are compared with the 3-D model. Figure 3 is the counterpart of Figure 2, but considers the M2D model. In both cases, it is easy to verify the benefits of adding terms in the relevant expansion series. Indeed, the

TABLE 6

First frequency parameters, ω^*, for orthotropic plates; [0/90/0/90°]; ($n = 1$)

	D2D, N							
L_x/h	1	3	5	7	PAR_{ds}	3-D	$e\%D2D_7$	$e\%$ PAR_{ds}
2·5	0·875924	0·806547	0·799598	0·792924	0·875924	0·779708	1·7	12·3
10	0·115672	0·111888	0·110865	0·110268	0·115672	0·109461	0·7	5·7
100	0·00133113	0·00133051	0·00133032	0·00133020	0·00133113	0·00133005	0·0	0·1
200	0·000333196	0·000333157	0·000333145	0·000333138	0·000333196	0·000333129	0·0	0·0
500	0·0000533300	0·0000533290	0·0000533287	0·0000533285	0·0000533300	0·0000533282	0·0	0·0
	M2D, N							
L_x/h	1	3	5	7	PAR_{cs}	3-D	$e\%M2D_7$	$e\%$ PAR_{cs}
2·5	0·802076	0·742103	0·768963	0·778136	0·831635	0·779708	− 0·2	6·7
10	0·113288	0·109150	0·108836	0·109239	0·112403	0·109461	− 0·2	2·7
100	0·00133076	0·00133003	0·00132994	0·00133001	0·00133059	0·00133005	0·0	0·0
200	0·000333173	0·000333127	0·000333121	0·000333126	0·000333162	0·000333129	0·0	0·0
500	0·0000533294	0·0000533282	0·0000533280	0·0000533282	0·0000533291	0·0000533282	0·0	0·0

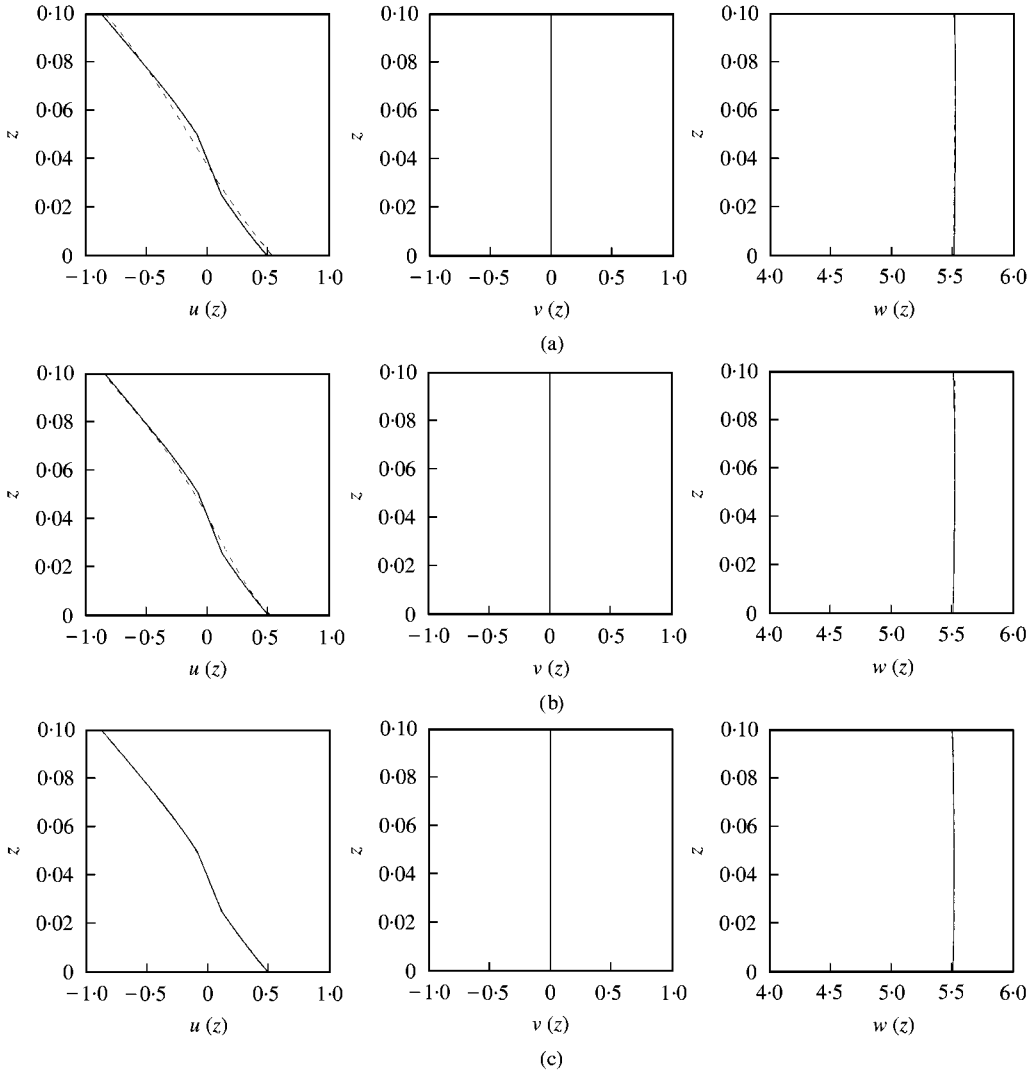

Figure 2. Mode shapes through the thickness of the laminate; reference Table 1; comparison: D2D–3-D; $n = 1$; [0/90/0/90°]. (a) 3-D (0·1094611), (- - -) PAR_{ds}(0·115672, + 5.7%); (b) 3-D (0·01094611), (- - -) D2D_2 (0·112590, + 2.9%); (c) 3-D (0·1094611), (- - -) D2D_8 (0·110153, + 0.6%).

displacements match the exact displacement distribution better as the number of terms increases. In particular, in Figures 2(c) and 3(c), where eight terms are used in the expansions, the 3-D mode and relevant 2-D ones are practically indistinguishable. However, the M2D model behaves better although the good agreement in displacements is comparable to the agreement present between D2D and 3-D. It, however, cannot be forgotten that the M2D goes beyond being a good approximation concerned with only the displacement. Figures 4 and 5 are extremely interesting with respect to the capability of both approaches to model quite accurately the displacement fields as the relevant expansion series increase. Particularly interesting are Figures 4(a) and 5(a) with respect to the distortions that PAR_{cs} and PAR_{ds} can introduce with respect to the true distribution of the in-plane displacements which, with a few layers and from a layout dependence, can be highly non-linear.

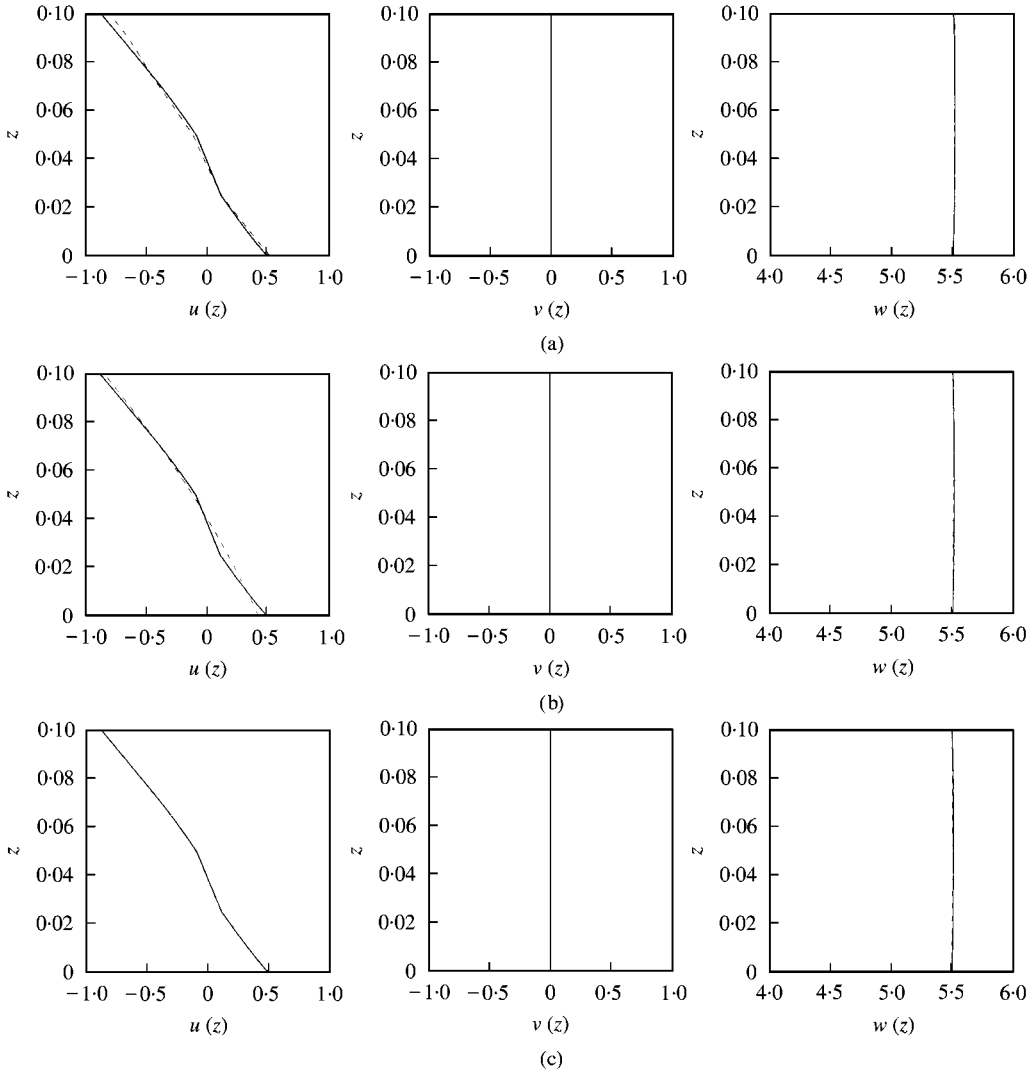

Figure 3. Mode shapes through the thickness of the laminate; reference Table 2; comparison: M2D–3-D; $n = 1$; [0/90/0/90°]. (a) 3-D (0·1094611), (- - -) PAR_{cs}(0·112403, + 2.7%); (b) 3-D (0·1094611), (- - -) M2D_2 (0·110066, + 0.6%); (c) 3-D (0·1094611), (- -) M2D_8 (0·109406, − 0.05%).

Finally, Figure 6 illustrates the case with a relatively high number of layers. The M2D, like the D2D, averages the real 3-D displacement distribution (a "zig–zag"), but unlike the D2D it quite accurately estimates the natural frequency. This is evidently attributed to the modelling of the transverse shear stress that fulfills the continuity requirements.

Graphic outputs, in conjunction with Tables 1 and 2, show that when a few layers constitute the laminate, the in-plane displacements can be highly non-linear or, at least, the displacements are not extremely well approximated by the cubic terms, layer by layer. The transverse section can then be distorted in such a way that a global average distribution of the in-plane displacements (PAR_{ds}) could transform the PAR_{ds} into a better model than PAR_{cs}. However, when the layers increase, a "zig-zag" distribution coming from PAR_{cs}

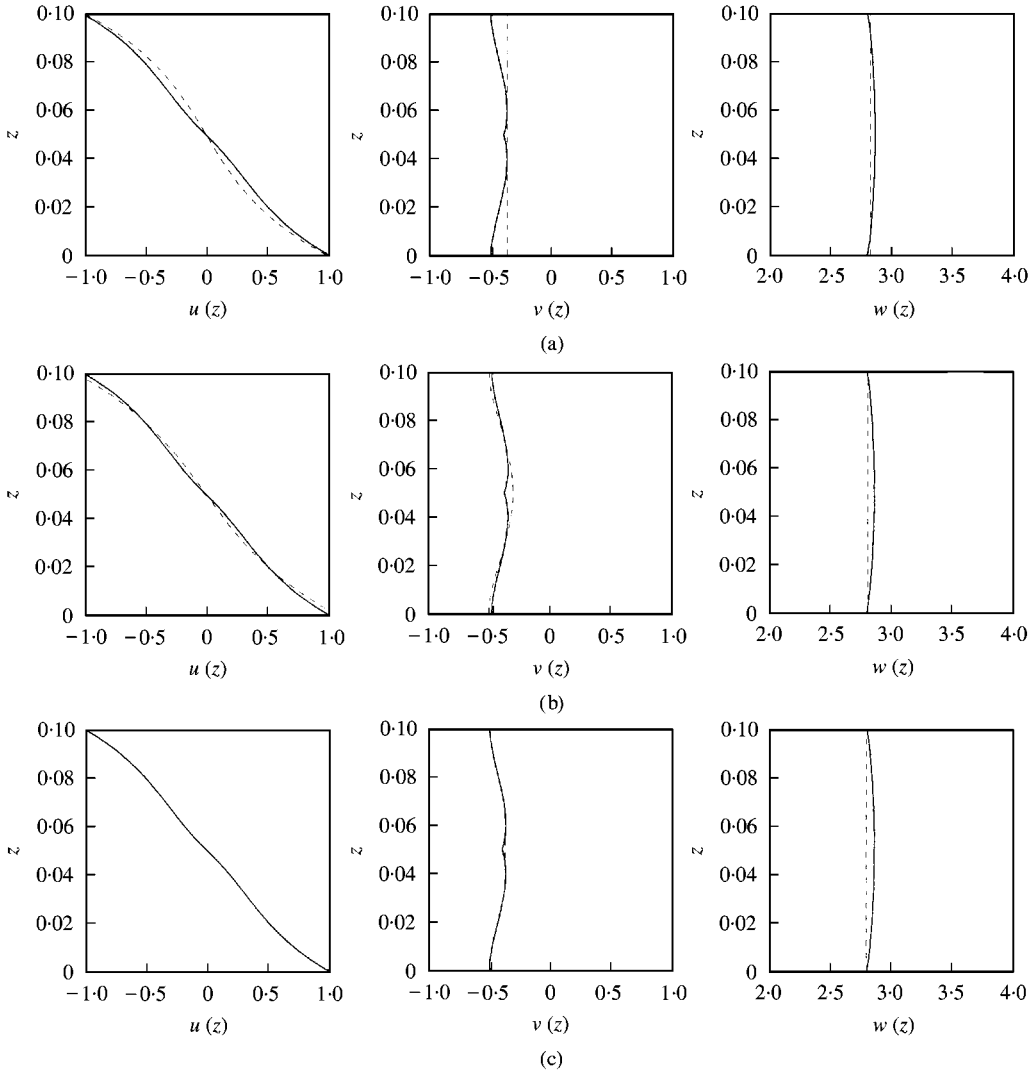

Figure 4. Mode shapes through the thickness of the laminate; [45/ − 45°]; comparison: D2D–3-D; $n = 4$; $h/L_x = 0.1$. (a) 3-D(0·7141170), (- - -) PAR_{ds}(0·737823, + 3.3%); (b) 3-D(0·7141170), (- - -) D2D_2 (0·724107, + 1.4%); (c) 3-D(0·7141170), (- - -) D2D_8 (0·714527, + 0·06%).

results in a better solution and even the M2D can constitute an appreciable solution for low and relatively high number of layers.

After discussing the numerical tables and graphical outputs it should be appreciated how different models, based on different substantial mathematical treatment, are going to give results in excellent agreement (3-D exact, the D2D by using a polynomial base with *extremum* at the ends, the M2D by using two different polynomial bases such as "completely free" for the displacement and "simply supported" for the transverse shear stress at the ends) in a refined and unified notation [equations (6)–(15) for the D2D along with equations (24)–(27) for the M2D]. Based on the simplicity of such an expansion-based method, it should be interesting to account for the normal effects. Its importance was considered elsewhere [30] in the case of a layer-wise description.

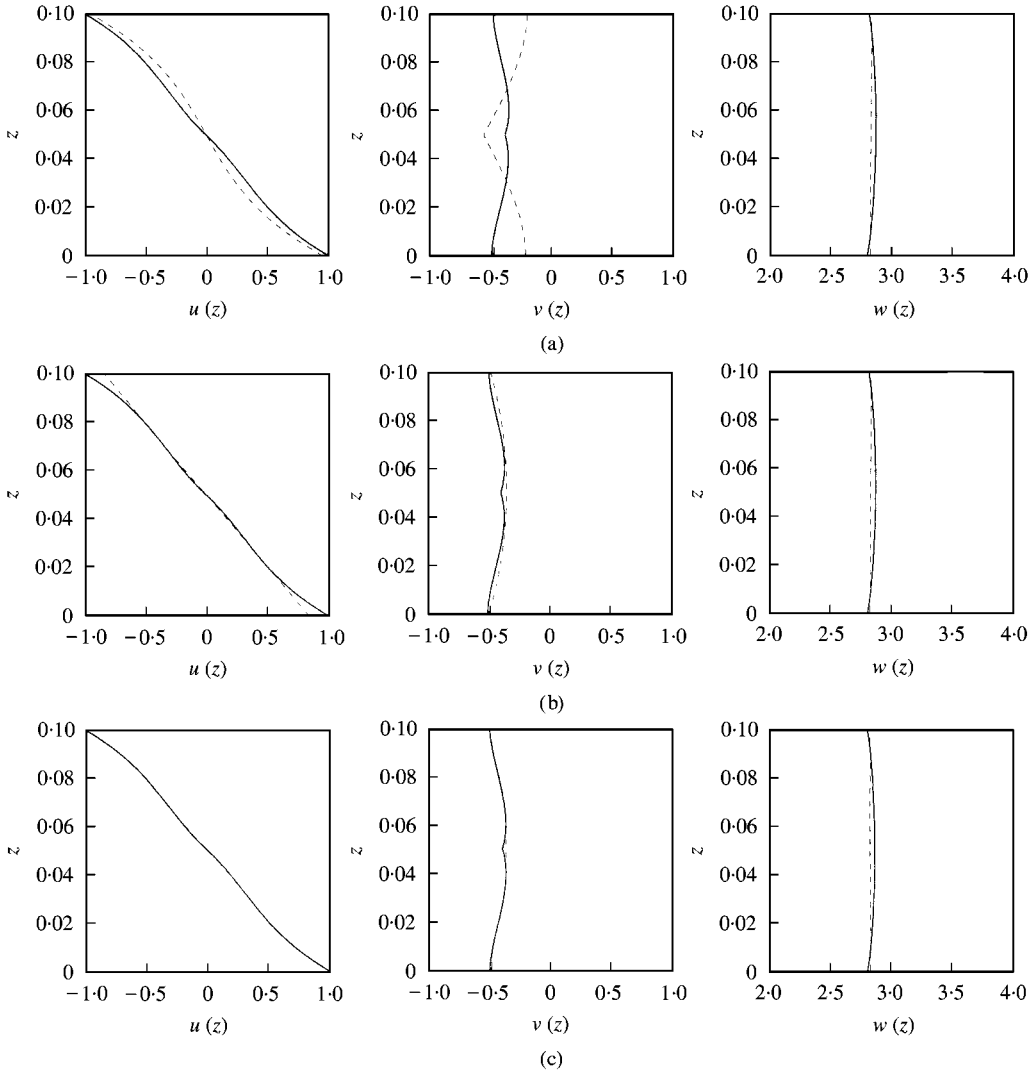

Figure 5. Mode shapes through the thickness of the laminate; [45/ − 45°]; comparison: M2D–3-D; $n = 4$; $h/L_x = 0{\cdot}1$. (a) 3-D(0·714117), (- - -) PAR_{cs}(0·804256, + 12.6%); (b) 3-D(0·714117), (- - -) M2D_2 (0·689217, − 3.5%); (c) 3-D(0·714117), (- -) M2D_8 (0·712842, − 0.18%).

5. CONCLUSIONS

This paper introduces, in a unified notation, two different generalized higher order theories extending 2-D models to account for arbitrarily high number of degrees of freedom for an accurate modelling for free vibration studies of composite multilayered plates. This generalization has been obtained by expanding in-plane displacements and stresses throughout the thickness of the laminate. An orthogonal base has been initially proposed obtaining a model (D2D) in accordance with displacement-based plate theories [1–3, 6] that violate the interlaminar continuity requirements concerned with the interlaminar transversal shear stresses. It is an extension of recent higher order theories and, besides their possible equivalencies [8], it has been presented mainly by referring to the notations used in references [6, 17, 18, 14] and herein indicated as PAR_{ds}. It has been numerically shown that

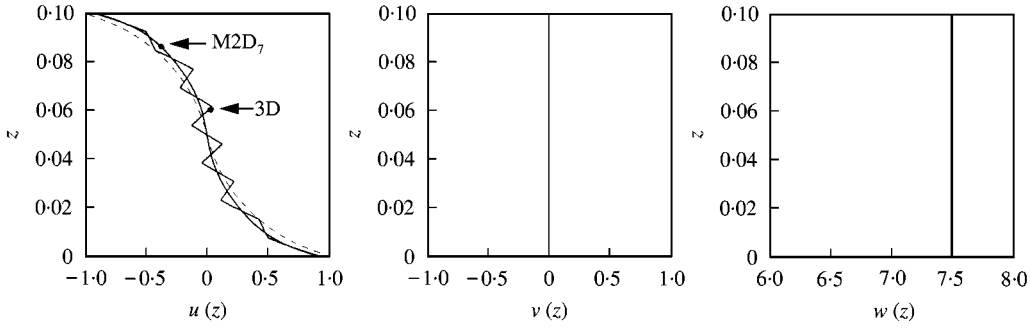

Figure 6. Mode shapes through the thickness of the laminate; $[(0/90^\circ)_3/0^\circ_1]_s$; comparison: D2D–M2D–3-D; $n = 3$; $h/L_x = 0{\cdot}1$. 3-D(0·611977), (- - -) D2D_7 (0·662178, + 8.2%), M2D_7 (0·611633, − 0.06%).

such a generalized displacement-based higher order model is able to improve the performance of its origin (PAR_{ds}) by numerical convergence tests. Such as improvement, however, seems to be layout-dependent.

A generalized model accounting in a weaker form for all the continuity requirements (in-plane displacements and transverse shear stresses are approximated as continuous functions with continuous derivatives) has also been introduced by using different bases with respect to the base used in the D2D model. This model (M2D) has been introduced in the light of a mixed approach where displacement and stress can be independently modelled. The presentation of this model (M2D) has been provided with respect to the 2-D generalized model violating the stress continuity requirements (D2D) in a unified notation to highlights the main relevant differences. The mixed plate model has then been tested against the displacement-based one and an excellent performance has been obtained compared to the 3-D results. Several numerical tests have shown the independence of the M2D model from the number of layers, the stacking lamination schemes and finally, from the lower and higher frequencies. Whenever the continuity requirements are absent an exact correspondence between D2D and M2D has been verified to demonstrate the invariance of the both models with respect to the physics of the problem. Due to the particular bases used, any complications, concerned with mathematical treatments at the interfaces or at the top and bottom of the laminate, to fulfil continuity requirements or traction boundary conditions, respectively, are not requested. Based on the engineering applications, it can be concluded that the M2D seems to be able to assess fairly satisfactorily natural frequencies and relevant modal data by using continuous functions to approximate in-plane displacements and transverse stresses. The overestimation and/or underestimation of natural frequencies, obtained from previous higher order theories, has been justified by using both the generalized models D2D and M2D.

The capability of such a mixed model to approach "asymptotically" the exact 3-D eigenvalues sounds extremely interesting. However, based on the comparison with a relevant 3-D code normal effects have been detected important for some higher frequencies, as has been highlighted, on the other hand, in reference [30]. It remains to verify whether a model accounting for such 'normal effects' together with fulfilling the continuity requirements, in a weaker form, is able to further improve the performance herein presented by the generalized M2D model.

REFERENCES

1. A. BHIMARADDI and L. K. STEVENS 1984 *Journal of Applied Mechanics* **51**, 195–198. A high-order theory for free vibration of orthotropic, homogeneous, and laminated rectangular plates.

2. J. N. REDDY 1984 *Journal of Applied Mechanics* **51**, 745–752. A simple higher-order theory for laminated composite plates.
3. J. N. REDDY and C. F. LIU 1985 *International Journal of Engineering Sciences* **23**, 319–330. A higher-order shear deformation theory of laminated elastic shells.
4. K. H. LO, R. M. CHRISTENSEN and E. M. WU 1977 *Journal of Applied Mechanics* **44**, 663–668. A high-order theory of plate deformation. Part 1: homogeneous plates.
5. K. H. LO, R. M. CHRISTENSEN and E. M. WU 1977 *Journal of Applied Mechanics* **44**, 669–676. A high-order theory of plate deformation. Part 2: laminated plates.
6. K. P. SOLDATOS 1987 *Journal of Sound and Vibration* **119**, 111–137. Influence of thickness shear deformation on free vibrations of rectangular plates, cylindrical panels and cylinders of antisymmetric angle-ply construction.
7. A. A. KHDEIR 1989 *Journal of Sound and Vibration* **128**, 377–395. Free vibration and buckling of unsymmetric cross-ply laminated plates using a refined theory.
8. J. N. REDDY 1990 *Meccanica* **25,** 230–238. On refined theories of composite laminates.
9. P. S. FREDERIKSEN 1995 *Journal of Sound and Vibration* **186**, 743–759. Single-layer plate theories applied to the flexural vibration of completely free thick laminates.
10. C. C. CHEN, K. M. LIEW, C. W. LIM and S. KITIPORNCHAI 1999 *Journal of Acoustical Society of America* **102**, 1600–1611. Vibration analysis of symmetrically laminated thick rectangular plates using the higher-order theory and p-Ritz method.
11. A. A. KHDEIR and J. N. REDDY 1999 *Computers and Structures* **71**, 617–626. Free vibrations of laminated composite plates using second-order shear deformation theory.
12. A. MESSINA, E. J. WILLIAMS and T. CONTURSI 1998 *Journal of Sound and Vibration*, **216**, 791–808. Structural damage detection by a sensitivity and statistical-based method.
13. A. MESSINA and E. J. WILLIAMS 1999 Second International Conference of Identification in Engineering Systems, *University of Wales, Swansea, U.K.*, 440–449. Use of changes in resonances and antiresonance frequencies for damage detection.
14. A. MESSINA and K. P. SOLDATOS 1999 *International Journal of Mechanical Sciences* **41**, 891–918. Vibration of completely free composite plates and cylindrical shell panels by a higher order theory.
15. A. MESSINA and K. P. SOLDATOS 1999 *Journal of Acoustical Society of America* **106**, 2608–2620. Influence of edge boundary conditions on the free vibrations of cross-ply laminated circular cylindrical panels.
16. A. MESSINA and K. P. SOLDATOS 2000 A general vibration model of angle-ply laminated plates that accounts for the continuity of interlaminar stresses (submitted).
17. K. P. SOLDATOS and T. TIMARCI 1993 *Composite Structures* **25**, 165–171. A unified formulation of laminated composite, shear deformable, five-degrees-of-freedom cylindrical shell theories.
18. T. TIMARCI and K. P. SOLDATOS 1995 *Journal of Sound and Vibration* **187**, 609–624. Comparative dynamic studies for symmetric cross-ply circular cylindrical shells on the basis of a unified shear deformable shell theory.
19. A. MESSINA and K. P. SOLDATOS 1999 *Journal of Sound and Vibration* **227**, 749–768. Ritz-type dynamic analysis of cross-ply laminated circular cylinders subjected to different boundary conditions.
20. L. LIBRESCU and W. LIN 1996 *European Journal of Mechanics A/Solids* **15**, 1095–1120. Two models of shear deformable laminated plates and shells and their use of prediction of global response behavior.
21. P. B. XAVIER, C. H. CHEW and K. H. LEE 1995 *International Journal Solids and Structures* **32**, 3479–3497. Buckling and vibration of multilayer orthotropic composite shells using a simple higher-order layerwise theory.
22. J. N. REDDY and N. D. PHAN 1985 *Journal of Sound and Vibration* **98**, 157–170. Stability and vibration of isotropic, orthotropic and laminated plates according to a higher order shear-deformation theory.
23. K. P. SOLDATOS 1992 *Composite Structures* **20**, 195–211. A general plate theory accounting for continuity of displacements and transverse shear stresses at material interfaces.
24. E. CARRERA 1997 *Composite Structures* **37**, 373–383. C_z^0 Requirements-models for the two dimensional analysis of multilayered structures.
25. H. MURAKAMI 1986 *Journal of Applied Mechanics* **53**, 661–666. Laminated composite plate theory with improved in-plane responses.
26. A. TOLEDANO and H. MURAKAMI 1987 *Journal of Applied Mechanics* **54**, 181–188. A composite plate theory for arbitrary laminate configurations.

27. M. E. Fares, M. N. M. Allam, and A. M. Zenkour 1989 *Solids Mech. Archives* **14**, 103–114. Hamilton's mixed variational formula for dynamical problems of anisotropic elastic bodies.
28. M. E. Fares 1999 *International Journal of Non-linear Mechanics* **34**, 685–691. Mixed variational formulation in geometrically non-linear elasticity and a generalized *n*th-order beam theory.
29. E. Carrera 1998 *Journal of Applied Mechanics* **23**, 820–828. Layer-wise mixed models for accurate vibration analysis of multilayered plates.
30. E. Carrera 1999 *Journal of Sound and Vibration* **225**, 803–829. A study of transverse normal stress effect on vibration of multilayered plates and shells.
31. E. Reissner 1950 *Journal of Mathematics and Physics* **29**, 90–95. On a variational theorem in elasticity.
32. E. Reissner 1986 *International Journal of Numerical Methods in Engineering* **23**, 193–198. On a mixed variational theorem and on shear deformable plate theory.
33. K. P. Soldatos 1995 *Journal of Sound and Vibration* **883**, 819–839. Generalization of variationally consistent plate theories on the basis of a vectorial formulation.
34. R. B. Bath 1985 *Journal of Sound and Vibration* **102**, 493–499. Natural frequencies of rectangular plates using characteristic orthogonal polynomials in Rayleigh–Ritz method.
35. J. Fan and J. Ye 1990 *International Journal of Solids and Structures* **26**, 655–662. An exact solution for the statics and dynamics of laminated thick plates with orthotropic layers.
36. J. Ye and K. P. Soldatos 1994 *Composite Engineering* **4**, 429–444. Three-dimensional vibration of laminated cylinders and cylindrical panels with symmetric or antisymmetric cross-ply lay-up.
37. A. K. Noor and W. S. Burton 1989 *Applied Mechanical Reviews* **42**, 1–13. Assessment of shear deformation theories for multilayered composite plates.
38. J. M. Whitney 1987 *Structural Analysis of Laminated Anisotropic Plates*. Lancaster: Technomic.
39. L. Meirovitch 1997 *Principles and Techniques of Vibrations*. London: Prentice-Hall.
40. N. J. Pagano 1970 *Journal of Composite Materials* **4**, 330–343. Influence of shear coupling in cylindrical bending of anisotropic laminates.